

## Turbulent flow through a plane sudden expansion

M. P. Escudier<sup>a</sup>, P. J. Oliveira<sup>b</sup> and R. J. Poole<sup>a</sup>

<sup>a</sup>University of Liverpool,  
Department of Engineering, Mechanical Engineering,  
Brownlow Hill, Liverpool, L69 3GH, UK

e-mail: [escudier@liv.ac.uk](mailto:escudier@liv.ac.uk)

e-mail: [robpoole@liv.ac.uk](mailto:robpoole@liv.ac.uk)

<sup>b</sup>Departamento de Engenharia Electromecânica,  
Universidade da Beira Interior, Rua Marquês D' Ávila e Bolama, 6200 Covilhã, Portugal

e-mail: [pjpo@ubi.pt](mailto:pjpo@ubi.pt)

### Abstract

The results are reported of an experimental investigation of turbulent flow through a plane sudden expansion of expansion ratio  $R=D/d=4$  and aspect ratio  $A=w/h=5.33$ . It is well known that plane sudden expansions with  $R$  greater than 1.5 produce asymmetric flows and this was again seen in this study. The literature for the asymmetric situation ( $R>1.5$ ) is surprisingly limited and only axial velocity and axial turbulence intensity results have been reported previously. A laser Doppler anemometer was used to measure mean and r.m.s axial velocities,  $U$  and  $u'$ , as well as the transverse r.m.s velocities,  $v'$ , and the Reynolds shear stress,  $\overline{uv}$ . Not only was the mean flow found to be asymmetric, but integration of the mean axial velocity profiles revealed significant departures from two dimensionality along the centreplane of the expansion duct. Results are reported at three spanwise locations to highlight this three dimensionality and qualitative arguments are made to relate this to the influence on corner vortices of the modest aspect ratio. A two-dimensional calculation method using the standard  $k-\epsilon$  turbulence model has been utilised to calculate the flow along the centreplane of the expansion. Despite the acknowledged deficiencies of the  $k-\epsilon$  model and the considerable deviation from two-dimensionality of the experimental flow, remarkably good agreement is found between the calculations and the measured centreplane flow structure.

## 1. Introduction

Turbulent flow through a plane sudden expansion is relevant to a number of important engineering applications including fluidic devices, heat exchangers, mixing equipment and air conditioning ducts. The number of investigations of turbulent flows through plane sudden expansions reported previously is surprisingly limited. A key geometric parameter is the expansion ratio  $R$  where  $R=D/d$ ,  $D$  being the downstream channel height and  $d$  the inlet height. Abbott and Kline (1962) were the first to investigate systematically the influence of  $R$  on flow through a plane sudden expansion. They found that for  $R > 1.5$  the flow became asymmetric with two recirculation zones of unequal length, while below this value the flow approached that for a double backward-facing step configuration with symmetrical regions of recirculation. They also observed that near reattachment the flow was not two-dimensional. The findings of Abbott and Kline (1962) have been confirmed by other investigators and it is now generally accepted that flow through a plane sudden expansion must be divided into two regimes depending on the expansion ratio. Tutu and Chevray (1975) and Eaton and Johnston (1981) have discussed the inadequacies of the hot-film technique used by Abbott and Kline (1962) for their turbulence measurements. In the present study, for which  $R=4$ , this lack of reliable data is addressed by including transverse velocities and turbulence intensities and the Reynolds shear stress together with the wall-pressure variation.

Restivo and Whitelaw (1978) were the first to investigate the asymmetric situation ( $R=3$ ) using laser Doppler anemometry (LDA). A major focus of their work was the turbulence energy spectrum which, they found, did not display significant peaks at the highest Reynolds number ( $Re=3995$ ). At lower Reynolds numbers, the energy spectra showed discrete peaks with relatively low energy at higher and lower frequencies. Limited profiles of axial velocity and turbulence intensity were reported for a Reynolds number of 2995. Although no mention is made in the paper itself of the two dimensionality of the flow, it is clear from the results that the flow rate, calculated by integrating velocity profiles, varies by up to 20% with axial location.

The most recent and relevant work to be reported is that of De Zilwa et al (2000) who presented LDA measurements of axial velocity and turbulence intensity for a duct with  $R=2.86$  and aspect ratio  $A=w/h=12.3$  at a Reynolds number of 26,500 together with numerical results based on the standard  $k - \epsilon$  method. The agreement between the experimental results and the numerical data is not completely satisfactory, the differences being attributed to deficiencies in the  $k - \epsilon$  method when dealing with turbulence anisotropy and streamline curvature. The flow is said to be two-dimensional over the middle 80% of the duct but the authors comment that integration of the velocity profile far downstream of the expansion showed a discrepancy of 15% compared with the measured flow rate.

The objective of the present paper is to investigate the assumption that nominally two-dimensional geometries produce two-dimensional flows. Previous papers which explore this topic have all been concerned with the two-dimensionality of flow behind backward-facing steps. de Brederode and Bradshaw (1972) studied the effects of small aspect ratio on the flow downstream of a backward-facing step using surface flow patterns and heat-transfer measurements. They concluded that the complicated stress-induced corner flows were confined to a distance of about 2 or 3 step heights from the sidewalls and that sidewall effects on the flow along the centreplane were negligible for aspect ratios greater than 10. Papadopoulos and Otugen (1995) investigated sidewall effects on the turbulent flow over a backward-facing step for a range of aspect ratios ( $1 < A < 28$ ) but their use of a hot-wire probe precluded measurements of the velocity within the recirculation region. From their measurements, combined with trends inferred from surface visualisation, Papadopoulos and Otugen concluded that the flow downstream of reattachment was three-dimensional.

## 2. Experimental rig and Instrumentation

The flow loop used for the present experiments was a modified version of that used by Escudier and Smith (2001) for their square-duct investigation. The square duct consisted of ten stainless steel modules each of length 1.2m and with an internal cross section of side length 80 mm. The plane sudden expansion, for which the key dimensions are given in **Figure 1**, replaced one of the existing modules 9.6 m from the inlet connection. The duct width  $w$  throughout is 80 mm, the inlet height  $d$  is 10 mm and the step height  $h$  is 15 mm. The downstream duct height  $D$  is 40 mm. The expansion was preceded by a short (53.5 mm in length), smooth contraction (40 mm radius followed by 20 mm radius) which led to a distribution of velocity at the plane of the sudden expansion which was practically uniform and of low turbulence intensity. The sidewalls of the expansion were made of borosilicate glass to permit velocity measurements using a laser Doppler anemometer. Distributions of mean velocity and turbulence structure were obtained from traverses at 13 axial locations (corresponding to  $x/d$  values of 0,1,2,3,4,5,6,7,10,12,15,18 and 21). These distributions were obtained at three spanwise locations,  $z/d=4, 1.5$  and  $6.5$ , which correspond to the XY-centreplane of the duct and one step height from each of the sidewalls (see **Figure 1**).

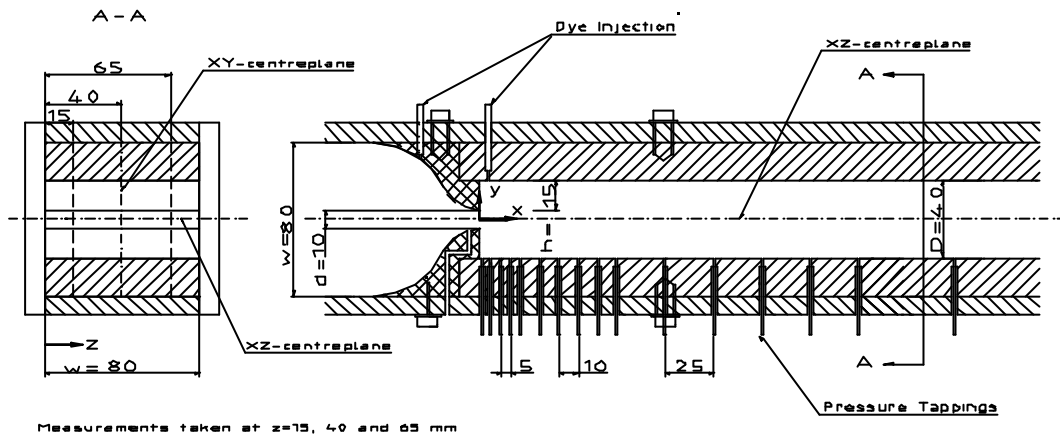


**Figure 1:** Plane sudden expansion geometry, dimensions in mm

A Dantec Fibreflow laser Doppler anemometer system was used for the velocity and turbulence measurements and comprised a Dantec 60X10 probe and a Dantec 55X12 beam expander in conjunction with two Dantec Burst Spectrum Analyzer signal processors (one model 57N10 the other model 57N20). The beam separation at the front lens was 51.5 mm and the lens focal length 160 mm which produces a measurement volume with principal axis of length 0.21 mm and diameter 0.025 mm. The axial and transverse velocity values were collected in coincidence to enable the Reynolds shear stress values to be estimated. As recommended by Tropea (1995) transit-time weighting was used to correct the velocity measurements for the effects of velocity bias. In view of the small diameter of the measuring volume, no correction was applied for the effect of velocity gradient broadening. Nominally 10,000 velocity samples were collected which resulted in a maximum relative statistical error, for a 95% confidence interval, of approximately 0.5% in the mean velocity and 1.4% in the turbulence intensity (Yanta and Smith (1978)).

As shown in **Figure 1**, 19 pressure tappings of 1 mm diameter were provided along the XY-centreplane of the expansion to allow the wall pressure variation to be measured. The tappings were connected to 2 mm ID clear vinyl tubing, filled with deionised water, linking each in turn via a series of valves to a Validyne differential pressure transducer (model DP15-26). Flow rates were measured using a Fischer and Porter electromagnetic flowmeter (model 10D1) incorporated in the flow loop upstream of the sudden expansion with the flowmeter output signal recorded via an Amplicon PS 30AT A/D converter.

The working fluid was filtered tap water with 100 ppm of 40% formaldehyde solution added to suppress bacterial activity. Approximately 0.25 gm of Timiron seeding particles were added to the fluid (total volume of fluid being 575 litres) to improve the LDA signal quality.

### 3. Numerical method

The two-dimensional equations of mean motion and those pertaining to the  $k - \epsilon$  turbulence model were solved using a finite-volume method using a non-staggered, and generally non-orthogonal, computational mesh which was deployed over the experimental test section. Details of the numerical procedure can be found in the work of Oliveira (1992) and Issa and Oliveira (1994). The plane just upstream of the converging section is treated as the computational inlet (subscript IN), where a uniform velocity profile is imposed  $U_{IN} = 0.7$  m/s together with uniform profiles for  $k$  and  $\epsilon$ . Values for these quantities were based on 2.5% turbulence intensity, giving  $k_{IN} = 4.41 \times 10^{-4} m^2 / s^2$ , while the dissipation was obtained from  $\epsilon_{IN} = k_{IN}^{1.5} / (0.1w)$ , giving  $\epsilon_{IN} = 1.15 \times 10^{-3} m^2 / s^3$ . A channel length of 500 mm was used in the simulations and a zero streamwise gradient condition ( $\partial / \partial x \equiv 0$ ) for all variables (including the pressure gradient) was applied at the outlet plane. As shown in **Figure 1** the origin of the Cartesian reference frame ( $x$  = axial,  $y$  = transverse) was placed at the nozzle mid-section. The remaining boundaries of the computational domain consisted of rigid walls at which the standard log-law treatment was employed (Launder and Spalding, 1975).

### 4. Results

All data presented here refer to a Reynolds number of 55,500 based on the mean bulk velocity at the inlet to the expansion ( $x/h=0$ ),  $U_B = 5.57$  m/s, and the duct height immediately upstream of the expansion,  $d=10$  mm. The heavy solid lines included in figures 2,3,6,7 and 8 showing the mean velocity and turbulence intensity distributions correspond to the numerical calculations.

#### 4.1. Wall-pressure variation

The flow asymmetry is apparent from the measured pressure distribution along the XY-centreplane of the duct for both top and bottom walls shown in **Figure 2**. The pressure within the shorter recirculation zone is much lower than in the longer. Since the shorter region of recirculation was equally likely to occur on the top and bottom walls, a pressure check was used to determine the flow configuration on start up and then, for consistency, the shorter region plotted as though occurring on the lower wall.

The pressure distribution on the upper wall closely resembles that found in a backward-facing step flow (see for example Chun and Sung, 1996). The pressure gradient on the lower wall is high immediately downstream of the expansion, the pressure reaching a maximum at the point where the flow reattaches (approximately  $x/d=5$ ). After the high velocity core of the shear layer impinges on the wall the pressure then falls until  $x/d=10$  whereafter the pressure has recovered significantly to become identical to that on the opposite wall.

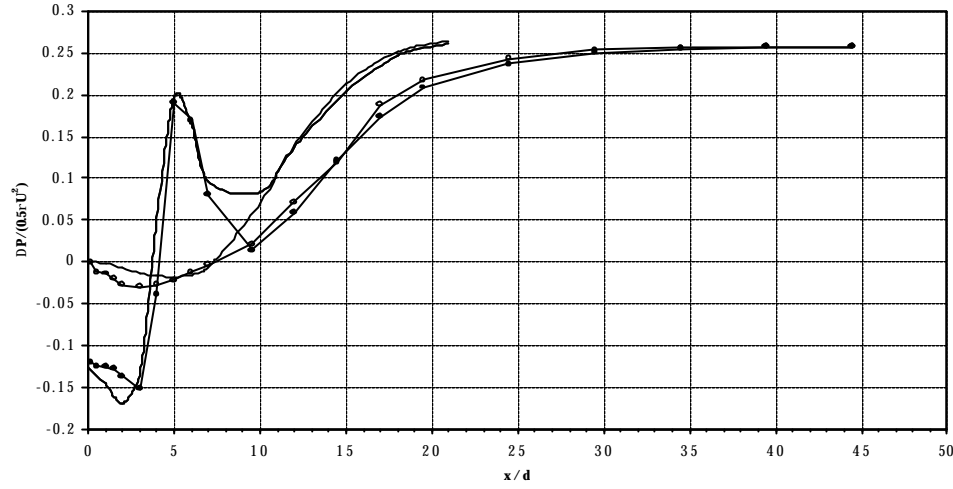


**Figure 2:** Wall pressure variation for the XY-centreplane ( ● lower side ○ upper side — k -ε model )

The calculated wall-pressure upstream of  $x/d=7$  is in good agreement with the experimental data, especially for the lower wall. The large pressure gradient on the lower wall is predicted well but after the maximum value is reached at  $x/d=5$  the calculated pressure falls below the experimental data. By  $x/d=10$  the calculated pressure is practically identical on both walls but is significantly higher than the experimental values.

#### 4.2. Mean axial velocity profiles, $U/U_B$

The mean axial velocity profiles of **Figure 3** are all asymmetric with unequal recirculation regions on the top and bottom walls in accordance with previous studies (see for example De Zilwa et al). Immediately apparent is that not only do the velocity profiles vary significantly across the span of the duct but also that they are not symmetrical about the XY-centreplane (i.e.  $z=40$  mm). This spanwise asymmetry is also confirmed, see **Table 1**, by the variation in the time averaged reattachment lengths for the three profiles. Due to the three-dimensional nature of the results, the stream function was not evaluated so that no streamline patterns can be presented. The flow field is clearly very complex with the profiles for  $z=40$  and 15 mm initially quite similar but with the peaks in the profiles for  $z=15$  mm following a slightly lower trajectory, impinging on the wall earlier and resulting in a shorter reattachment length,  $x_{RL}$ , about 20% lower than the for the XY-centreplane. The profile on the  $z=65$  mm side of the duct follows a significantly different development with its maximum velocity located nearer the XZ-centreplane resulting in an increase of the reattachment distance compared to the XY-centreplane of about 20%.

**Table 1:** Measured reattachment lengths and representative turbulence properties at different spanwise locations.

$z$ (mm)	$x_{RL}$ (x/d)	$x_{RU}$ (x/d)	$\frac{u'_{MAXL}}{U_B}$	$\frac{u'_{MAXU}}{U_B}$	$\frac{v'_{MAXL}}{U_B}$	$\frac{v'_{MAXU}}{U_B}$	$\frac{\overline{uv}_{MAXL}}{U_B^2}$	$\frac{\overline{uv}_{MAXU}}{U_B^2}$
15	3.7	20	0.219	0.245	0.183	0.136	0.0235	0.0109
40	4.7	17.3	0.216	0.261	0.191	0.143	0.0227	0.0119
65	5.6	17.5	0.229	0.218	0.161	0.131	0.0219	0.0106

The differences across the duct in the longer recirculation region are less pronounced than in the shorter and are again related to the location of the shear layer that is, in itself, determined by the trajectory of the

high velocity core. The lower trajectory of the  $z=15$  mm profiles has the inverse effect on the upper wall, namely to increase the reattachment distance relative to the XY-centreplane by approximately 15%. Close to the wall, between  $x/d=4$  and 12, the profiles at  $z=15$  and 40 mm are very similar until the longer recirculation region for  $z=15$  mm becomes evident. The axial velocity on the  $z=65$  mm side is positive immediately after the expansion and separation from the upper wall does not occur until  $x/d=5$ , after which the profiles resemble those at  $z=15$  and 40 mm before the flow reattaches at approximately the same location as for the XY-centreplane. Also, as Spazzini et al (2001) and others have found in studies of flow over a backward-facing step, it was observed that the reattachment lengths varied with time. Spectral analysis of the data revealed a significant peak at a distinct frequency of  $f \cong 8.16$  Hz ( $fh/U_B \cong 0.022$ ).

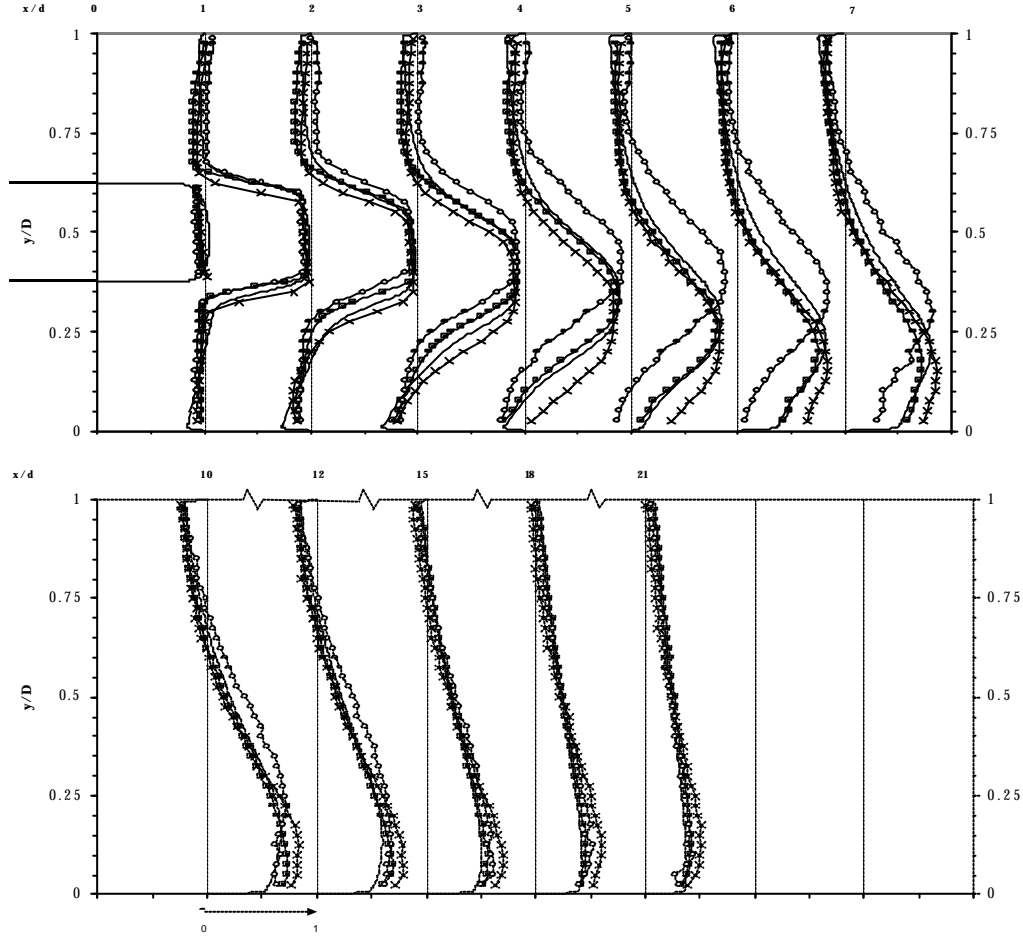


**Figure 3:** Mean axial velocity profiles ( $U/U_B$ ) for three XY planes  $\times$   $z=15$  mm  $\blacksquare$   $z=40$  mm  $\circ$   $z=65$  mm  
—  $k-\epsilon$  model

**Figure 3** shows that as the flow progresses downstream the differences diminish and the flow develops a more two-dimensional nature. By  $x/d=21$  the differences in the velocity profile across the duct are slight although the flow is still asymmetric from top to bottom, showing that the effect of the expansion is still being felt by the flow.

The good agreement between the calculations and the experimental data is remarkable considering both the acknowledged deficiencies of the  $k-\epsilon$  model (see for example De Zilwa et al) and the three dimensional nature of the experimental results. The location of the maximum velocity is well represented and the agreement between the calculated and measured reattachment lengths is very good. The predicted

reattachment lengths were equal to 4.65 and 16.6 inlet heights, which can be compared with the experimental values of 4.7 and 17.3.

To investigate flow two-dimensionality, each of the mean axial velocity profiles was integrated numerically producing the results seen in **Figure 4**. Also plotted is the average of the three apparent flow rates as a means of gross comparison. The figure reveals deviations from two-dimensionality of up to 20% downstream of the expansion. Upstream of  $x/d=15$  the flow rate is as much as 20% below that expected along the XY-centreplane of the duct which is surprising, as it would be expected that the sidewall boundary layers would retard the flow nearest the sidewalls and accelerate the flow in the XY-centreplane of the duct. In fact, just the opposite behaviour can be inferred from **Figure 4** with higher bulk velocities close to the sidewalls and low velocities in the XY-centreplane. By  $x/d=21$  the three flow rates are within 5% of each other and the value from the flowmeter. Since the velocity profile upstream of the contraction was measured and found to be symmetric, it must be the case that departures from two-dimensionality develop as a consequence of flow processes occurring within the duct itself.

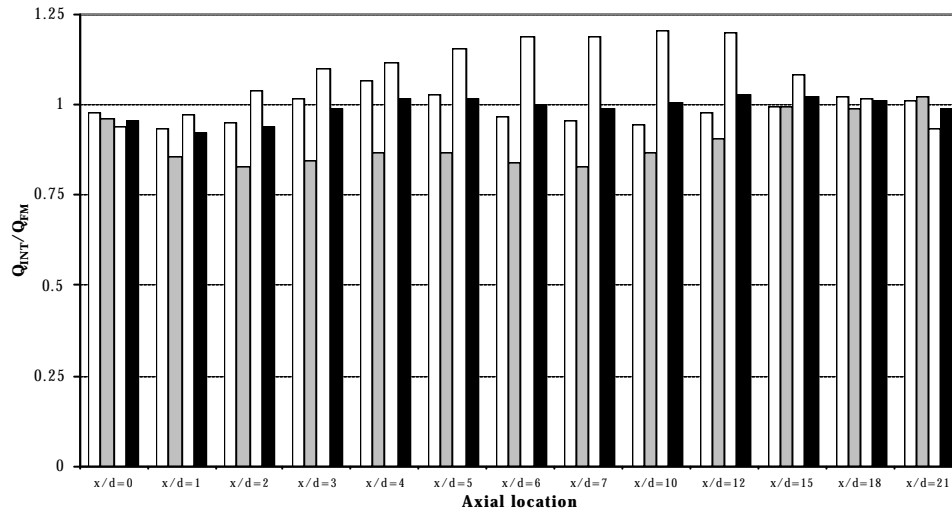


**Figure 4:** Comparison between flowrate from flowmeter and from integration of velocity profile ( $z=15, 40$  and  $65$  mm and average)

Immediately after the step, two opposing mechanisms appear to be acting in the upper and lower recirculation zones. In the upper region, the flow is reversed on the  $z=15$  mm side and in the centre but is in the positive streamwise direction on the  $z=65$  mm side indicating that there must be a spanwise velocity directed from  $z=15$  to  $65$  mm. For the lower region the flow rate is highest along the  $z=15$  mm side, resulting in the earlier reattachment on this surface, indicating that there is a spanwise velocity directed from  $z=65$  to  $15$  mm. According to Abbott and Kline, immediately after a step there is a three-dimensional zone of separation characterised by two, or more, vortices counter-rotating about axes parallel to the floor. It seems that the modest aspect ratio (5.33) in the current study has resulted in these two corner vortices being forced together resulting in destructive interference to produce a clockwise vortex on the lower wall and an anticlockwise vortex on the upper wall. It is this mechanism which causes the asymmetry about the XY-centreplane. To investigate this hypothesis the spanwise variation of the mean axial velocity component was measured at various transverse heights at  $x/d=2$ , the location of maximum flowrate deviation (**Figure 5**). Note that  $y$  is measured from the lower wall so that  $0 < y/D < 0.5$  corresponds to the lower half of the duct and  $0.5 < y/D < 1$  to the upper half. In the near-wall region ( $y/D < 0.2$ ) of the lower recirculation region shown in **Figure 5** all velocities are low in magnitude ( $< 0.2U_B$ ), negative and the flow is approximately two-dimensional as is the case in the high-velocity core ( $0.4 < y/D < 0.5$ ,  $U/U_B \approx 0.95U_B$ ). However for the shear layer in between, the flow is strongly skewed with higher velocities occurring on the near side of the expansion ( $0.2 < z/w < 0.4$ ) and a gradual decrease for  $z/w \rightarrow 1$ . The flow in the upper part of the duct is considerably more complicated, with the flow being strongly skewed not only within the shear

layer but also on the far side of the duct ( $z/w > 0.75$ ) where the flow changes from the negative to the positive streamwise direction, as was observed previously (**Figure 3**). Also, the spanwise asymmetry is in the opposite sense to the lower region with increased velocities on the far side of the duct.

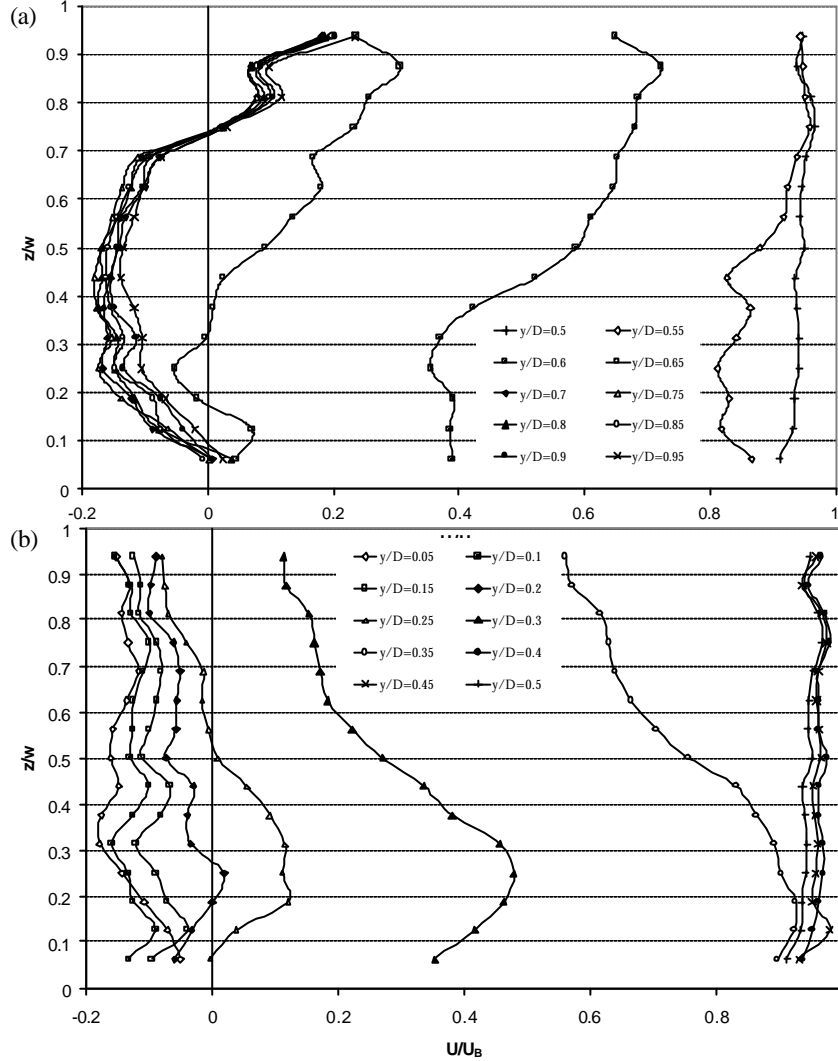


**Figure 5:** Spanwise variation of mean axial velocity profiles ( $U/U_B$ ) at  $x/d=2$  for various heights ( $y/D$ ) (a) above and (b) below the XZ-centreplane

#### 4.3. Axial turbulence intensity, $u'/U_b$

As can be seen in **Figure 6**, the asymmetry of the flow leads to the shear layers having different maximum values for the turbulence intensity and for these maxima to be located at different downstream locations. In the lower recirculation region the maxima follow the trajectory of the high velocity core towards the lower wall. In the upper half of the duct, the location of the local maximum moved towards and then below the XZ-centreplane, where the region of high turbulence intensity increases with shear layer growth. By  $x/d=10$  the upper and lower shear layers have merged and there is only one maximum value, located at approximately  $y/D = 0.5$ . After reattachment the  $u'_{MAX}/U_B$  values decrease rapidly as is also found in backward-facing step flows (see Eaton and Johnston). In the upper half of the duct the data again collapse quite well, still normalised by the lower reattachment distance, showing an increase in intensity until



reaching a maximum about one inlet diameter either side of the corresponding reattachment location. The  $z=15$  and  $40$  mm profiles have slightly higher values of maximum intensity in the upper recirculation region, 25-26%, compared to the lower. The  $z=65$  mm profile, with its more central trajectory, and hence similar sized shear layers, has roughly equal maxima in both.

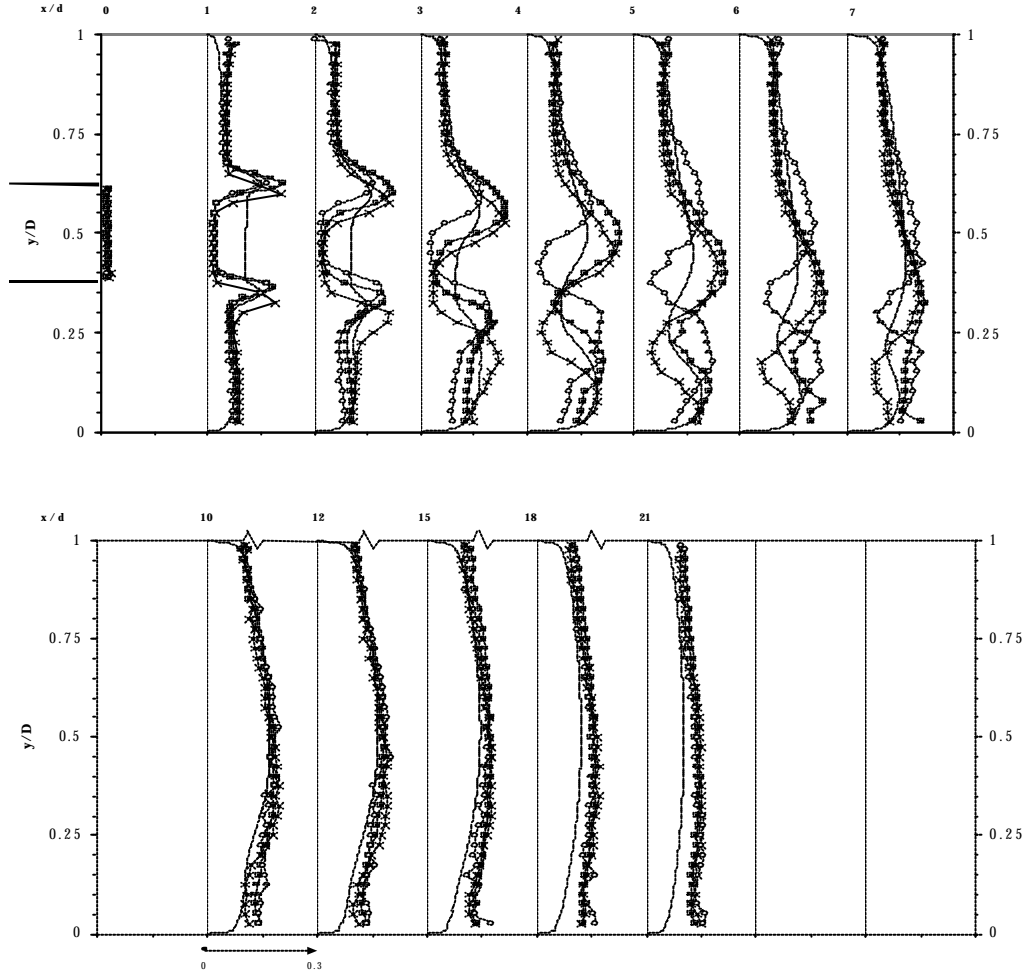


**Figure 6:** RMS axial turbulence intensity profiles ( $u'/U_B$ ) for three XY-planes  $\times z=15$  mm ■  $z=40$  mm ○  $z=65$  mm —  $k-\epsilon$  model

Since an underlying assumption of the standard  $k-\epsilon$  model is that the turbulence is isotropic, the turbulence intensity calculations are compared only with the axial turbulence intensity. The poor agreement between the calculated values and measured data is perhaps only to be expected when consideration is paid to the strongly anisotropic character of the turbulence within the recirculation regions. In the lower recirculation region, where the anisotropy is weaker, the agreement is more satisfactory but the peak values are under-predicted. In the upper recirculation region, the maximum values are also consistently under-predicted. Even at  $x/d=21$  the calculated intensities lie significantly below the measured axial intensities and this discrepancy is again attributable to anisotropy since the measurements show  $u'/v' \approx 1.33$  on the XZ-centreplane.

#### 4.4. Transverse turbulence intensity, $v'/U_B$

The profiles of transverse turbulence intensity shown in **Figure 7** are very similar in shape to those of the axial turbulence intensity but have consistently lower peak maximum intensities. Only in the low turbulence intensity core, between the two shear layers, is the turbulence practically isotropic. At all other locations  $v'$  is always lower than  $u'$ . This anisotropy is especially pronounced in the upper recirculation region where the peak values are significantly lower than their axial counterparts: 14% compared with 26%.

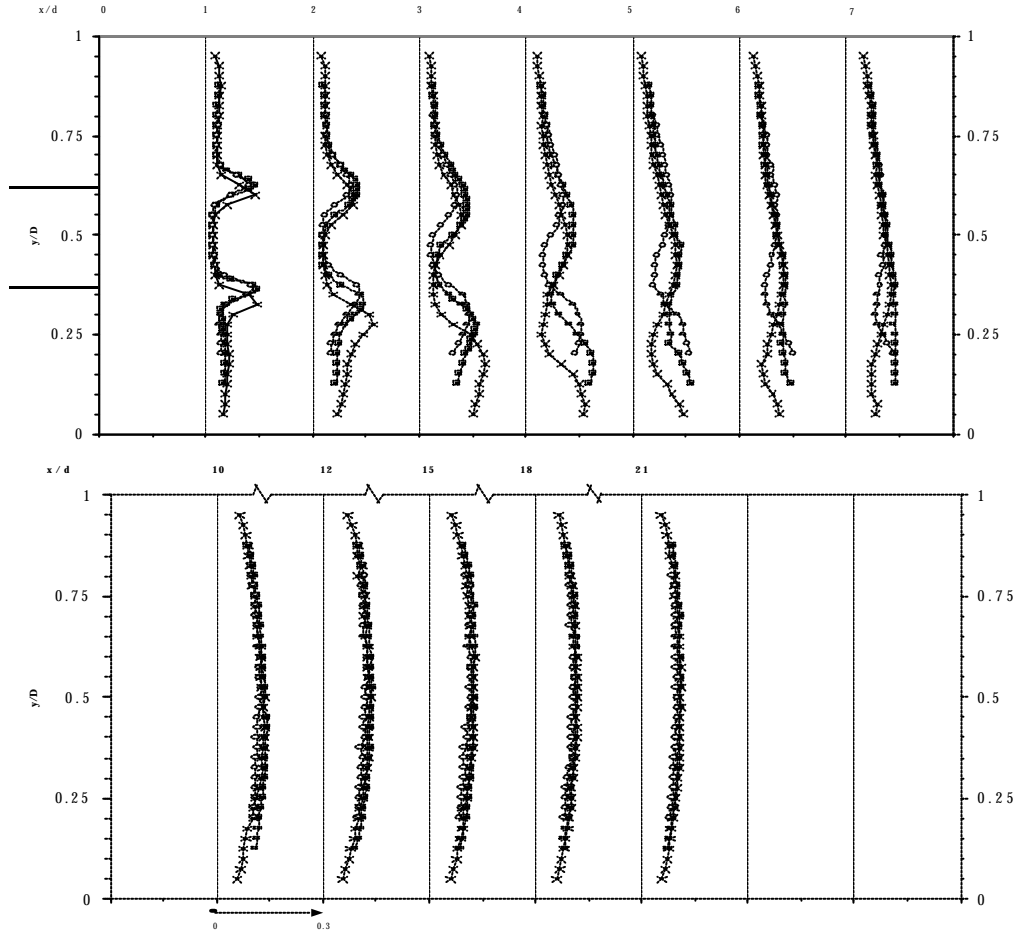


**Figure 7:** RMS radial turbulence intensity profiles ( $v'/U_B$ ) for three XY-planes  $\times$   $z=15$  mm  $\blacksquare$   $z=40$  mm  $\circ$   $z=65$  mm —  $k-\epsilon$  model

#### 4.5. Reynolds shear stress, $\overline{u'v'}/U_B^2$

The distribution of the Reynolds shear stress  $\overline{u'v'}$  is shown in **Figure 8**. Initially all three profiles,  $z=15$ , 40 and 65 mm, are very similar in shape but the  $z=15$  mm profile is shifted down towards the lower wall. By  $x/d=3$ , the  $z=40$  and 65 mm profiles have drifted apart, with the  $z=40$  mm profile peak value below the  $z=65$  mm profile again in accordance with the differing reattachment lengths (see **Table 1**). In the lower separation region the shear stress increases to a maximum,  $-\overline{u'v'}_{MAX} = 23 \times 10^3 U_B^2$ , at the edge of the recirculation zone with the peak occurring at the same axial location as the peak turbulence intensity. In

the upper recirculation region the maximum occurred immediately after the step and its value was roughly half that in the lower recirculation region, approximately  $11 \times 10^{-3} U_B^2$ . The peak of maximum shear stress decreases with downstream distance until at  $x/d=21$  the profile is almost symmetric with a gradual increase from zero at the wall to about  $-6 \times 10^{-3} U_B^2$  at the XZ-centreplane.

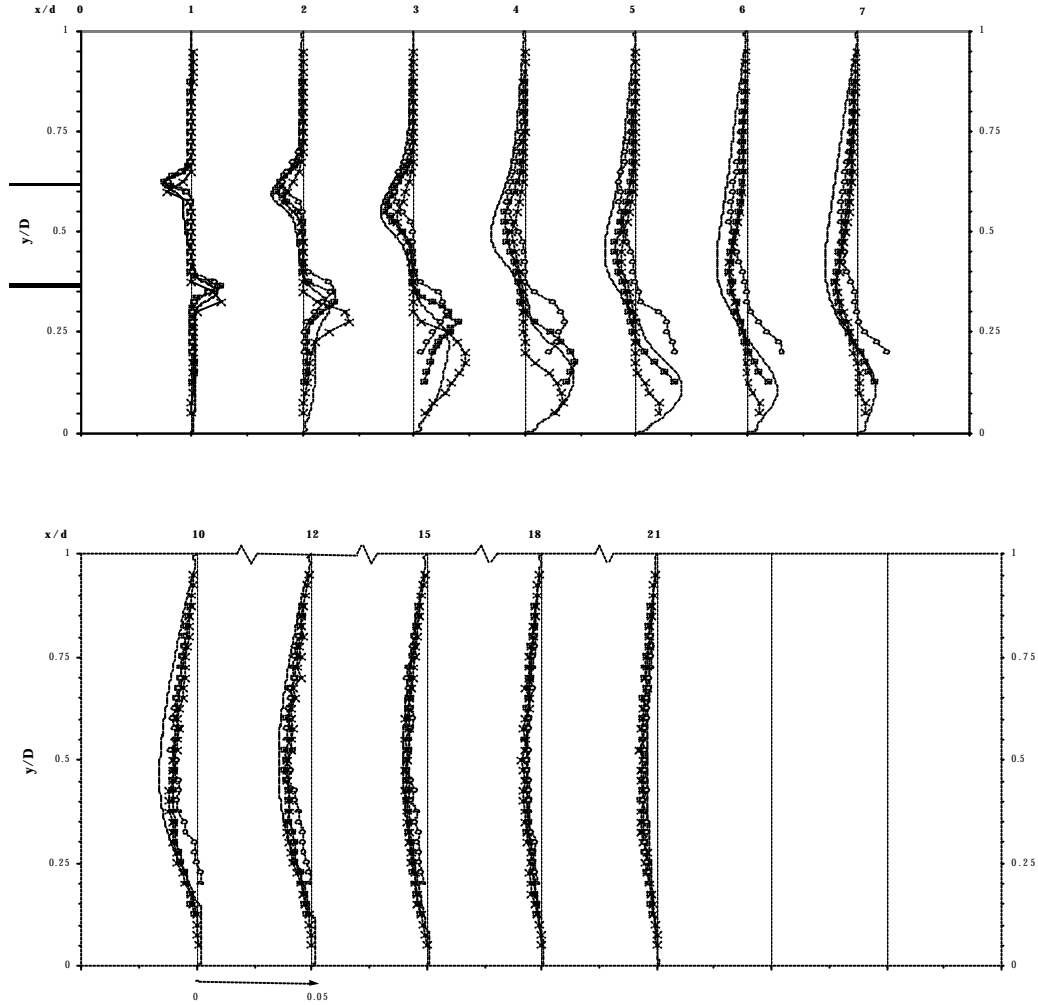


**Figure 8:** Reynolds shear stress profiles ( $-uv/U_B^2$ ) for three XY-planes  $\times$   $z=15$  mm  $\blacksquare$   $z=40$  mm  $\circ$   $z=65$  mm —  $k-\epsilon$  model

In contrast to the turbulence intensities, the predicted distribution of Reynolds shear stress better captures the qualitative trend of the experimental data. At the farthest downstream measurement location,  $x/d=21$ , the position of the maximum calculated value is on the XZ-centreplane, in agreement with the measurements. The value of the calculated shear stress at this point however is 30% lower than the corresponding experimental value. This difference indicates that the calculation predicts a more rapid decay of the shear stress with downstream location than the measurements.

## 5. Conclusions

Mean axial velocities, axial and transverse turbulence intensities and the Reynolds shear stress  $\overline{uv}$  together with the wall pressure variation have been reported for a plane sudden expansion, of expansion ratio 4, at three spanwise and 13 axial locations. Comparison with a two-dimensional numerical calculation, based on the standard  $k - \epsilon$  model, has also been presented.

In agreement with previous studies, the flow pattern downstream of the expansion was found to be asymmetric. Significant departures from two-dimensionality were observed along the XY-centreplane of the duct. It is suggested that the modest aspect ratio of 5.33 resulted in the two corner vortices formed just downstream of the expansion inlet being forced close together leading to the destructive interference of the two. This mechanism caused the flow to be asymmetric about the spanwise centreplane.

The maximum axial turbulence intensity occurred in the upper recirculation region with values as high as 26% of the bulk velocity at inlet while the maximum transverse intensity at this location was only 14%. Such strong anisotropy of the Reynolds normal stresses was not seen in the lower recirculation region where the intensities were roughly equal at about 20%. The maximum Reynolds shear stress  $-\overline{uv}/U_b^2$  measured was approximately  $23 \times 10^{-3}$  and this occurred in the lower recirculation region.

The two-dimensional numerical prediction showed remarkably good agreement with the mean axial velocity profiles. Agreement with the experimental reattachment lengths was also very good and within 5%. The turbulence properties were less well predicted as a consequence of the strongly anisotropic character of the actual flow and also its three dimensionality.

At  $x/d=21$  the flow had become essentially two-dimensional across the duct but was still asymmetrical about the XZ-centreplane showing that the flow had still not fully recovered from the effect of the inlet expansion.

## References

- D E Abbott, S J Kline, Experimental investigation of subsonic turbulent flow over single and double backward facing steps, *J. Basic Eng.* D84 (1962) 317.
- K B Chun, H J Sung, Control of turbulent separated flow over a backward-facing step by local forcing, *Exp. Fluids* **21** (1996) 417.
- V de Brederode, P Bradshaw, Three-dimensional flow in nominally two-dimensional separation bubbles; I. Flow behind a rearward facing step, *Aero Rep.* 72-19 (Imperial College of Science and Technology, London, England, 1972)
- S R N De Zilwa, L Khezzar, J H Whitelaw, Flows through plane sudden-expansions, *Int. J. Num. Meth. Fluids* **32** (2000) 313.
- J K Eaton, J P Johnston, A review of research on subsonic turbulent flow reattachment, *AIAA J.* **19** (1981) 1093.
- M P Escudier, S Smith, Fully developed turbulent flow of non-Newtonian liquids through a square duct, *Proc. R. Soc. London, Ser. A* 457 (2001) 911.
- R I Issa, P J Oliveira, Numerical prediction of phase separation in two-phase flow through T-Junctions, *Comput. Fluids* **23**, 347 (1994).
- B E Launder, D B Spalding, The numerical computation of turbulent flows, *Comput. Meth. Appl. Mech. Eng.* **3** (1975) 269.
- P J Oliveira, Computer modelling of multidimensional multiphase flow and application to T-Junctions, Ph.D. Thesis, Imperial College, University of London, 1992.
- G Papadopoulos, M V Otugen, Separating and reattaching flow structure in a suddenly expanding rectangular duct, *J. Fluids Eng.* 117 (1995) 17.
- A Restivo, J H Whitelaw, Turbulence characteristics of the flow downstream of a symmetric plane sudden expansion, *J. Fluids Eng.* 100 (1978) 308.
- P G Spazzini, G Iuso, M Onorato, N Zurlo, G M Di Cicca, Unsteady behavior of back-facing step flow, *Exp. Fluids* **30** (2001) 551.
- C Tropea, Laser Doppler anemometry: recent developments and future challenges, *Meas. Sci. Technol.* **6** (1995) 605.
- N K Tutu, R Chevray, Cross-wire anemometry in high-intensity turbulence, *J. Fluid Mech.* **74** (1975) 785.
- W J Yanta, R A Smith, Measurements of turbulence-transport properties with a laser-Doppler velocimeter, in *11<sup>th</sup> Aerospace Science Meeting*, (Washington, AIAA paper 73, 1978), p.169.